Uncertainty estimation of well catchments in heterogeneous aquifers

Fritz Stauffer, Sabine Attinger, Stephanie Zimmermann, and Wolfgang Kinzelbach
Institute of Hydromechanics and Water Resources Management, ETH Zurich, Switzerland

Received 27 July 2001; revised 23 May 2002; accepted 10 June 2002; published 15 November 2002.

[1] The uncertainty in the boundary of two-dimensional, steady state well catchments due to the uncertainty of the spatially variable hydraulic conductivity field is investigated. The well discharge rate and the areal recharge rate are assumed constant. The catchment boundary is traced by backward particle tracking in the velocity field. The uncertainty bandwidth of the catchment boundary is approximated in first order by formulating the time-dependent longitudinal and transversal second moments of the particle displacements along and normal to the mean particle trajectory. Applications of the approach are presented for a set of simple configurations. The results are compared with the results from unconditional numerical Monte Carlo simulations. The comparison allows an assessment of the accuracy, the applicability, and the limits of the method. The approximation corresponds quite well with the Monte Carlo simulations provided that the distance to the domain boundary is sufficiently large. *INDEX TERMS:* 1832 Hydrology: Groundwater transport; 1829 Hydrology: Groundwater hydrology; 1869 Hydrology: Stochastic processes; 3210 Mathematical Geophysics: Modeling; *KEYWORDS:* groundwater, protection zones, transport processes, modeling, uncertainty estimation, stochastic processes

Citation: Stauffer, F., S. Attinger, S. Zimmermann, and W. Kinzelbach, Uncertainty estimation of well catchments in heterogeneous aquifers, *Water Resour. Res.*, *38*(11), 1238, doi:10.1029/2001WR000819, 2002.

1. Introduction

[2] Regulations for the protection of water resources require the designation of recharge areas of pumping wells, which are endangered by pollution. The recharge area is related to the well catchment or wellhead protection zone. However, the practical determination of well catchments is often hampered by a series of considerable problems. One of these problems is the scarcity of observations within the well catchment. Together with the more or less highly heterogeneous nature of aquifer parameters only estimates of the location of the well catchment boundary can be given. Such estimates should be supplemented by the probability estimation of a particular location to belong to the catchment. A fully related question is to estimate the uncertainty bandwidth of the location of the catchment boundary.

[3] A large number of numerical methods and related codes have been developed, which can be used to determine well catchments [e.g., *Kinzelbach et al.*, 1992]. The question of uncertainty in the determination of well catchments and time-related capture zones due to the spatial variability in aquifer parameters has been raised by *Varljen and Schafer* [1991] and *Vassolo et al.* [1998] and solved by stochastic analysis using a numerical Monte Carlo technique. Numerical Monte Carlo techniques in connection with well catchments and time-related capture zones have been further developed by *Franzetti and Guadagnini* [1996], *Van Leeuwen et al.* [1998, 2000], *Guadagnini and Franzetti* [1999], *Riva et al.* [1999], and *Feyen et al.* [2001]. Monte Carlo type techniques are important stochastic tools for the demonstration of the impact of aquifer heterogeneity and uncertainty in boundary conditions. Moreover, they allow valuable comparisons of the results with alternative approximations. However, due to their high demand of computer time, there is a need for less expensive alternatives for a practical assessment of the uncertainty of well catchments and capture zones.

[4] The aim of the present paper is to estimate the uncertainty of the location of a well catchment boundary, given the uncertainty of the spatially variable hydraulic conductivity field and using a first-order approximation. The following assumptions are adopted for reasons of simplicity: (1) The aquifer can be modeled as a horizontally plane system. (2) The aquifer consists of one layer, which may be confined or unconfined. (3) The flow field is at steady state. (4) The well discharge rate is constant. (5) The areal recharge rate (natural recharge) is constant and is homogeneously distributed over the well catchment and its surroundings. (6) The expected average flow field can be calculated by using a constant effective hydraulic conductivity corresponding to the geometric mean. (7) The catchment boundary and its uncertainty can be determined by considering only the advective transport mechanism, thus neglecting local dispersion and molecular diffusion. (8) The spatial variability of the natural logarithm of hydraulic conductivity can be described by its variance and correlation length (integral scale) adopting an exponential covariance function.

[5] The restriction to two-dimensional flow conditions is justified for catchments of fully penetrating wells with large pumping rate Q_w, small recharge rate N, small distance between well and upstream boundary w, and small aquifer thickness H, according to the criterion $\kappa = Q_w/(N\ w\ H)>5$ [*Kinzelbach et al.*, 1992].

0043-1397/02/2001WR000819$09.00

[6] The analysis in this paper is based on a steady state reverse velocity field. The boundary of the well catchment is thus determined by the backward movement of two single particles in the heterogeneous velocity field, starting near the stagnation point of the well. Many realizations should lead to an assessment of the uncertainty of the catchment boundary by analyzing the ensemble of particle tracks. The uncertainty of the catchment boundary is approximated by the time-dependent longitudinal and transversal second moments of the particle displacements, along and normal to the mean particle trajectory.

2. Lagrangian Approximation of the Uncertainty in the Location of Well Catchment Boundaries

2.1. Problem Statement

[7] The steady state flow problem requires the solution of the following equation:

$$\nabla \cdot [(K(\mathbf{x})H(\mathbf{x}))\nabla h(\mathbf{x})] + N = -\nabla \cdot [\mathbf{q}(\mathbf{x})H(\mathbf{x})] + N = 0 \quad (1)$$

where $K(\mathbf{x})$ is the hydraulic conductivity, which is variable in space $\mathbf{x}$, and $H(\mathbf{x})$ is the saturated aquifer thickness. The variable $h(\mathbf{x})$ is the hydraulic head, $\mathbf{q}(\mathbf{x})$ is the (vertically averaged) specific flux vector, and N is the areal recharge rate, which is taken as constant. The hydraulic conductivity $K(\mathbf{x})$ is assumed to obey a spatial correlation function according to an isotropic exponential covariance function $C_Y(\mathbf{r}) = \sigma_Y^2 \exp(-|\mathbf{r}|/I_Y)$ with $Y = \ln(K)$. Standard boundary conditions are adopted. A pumping well with the pumping rate Q_w is located at $\mathbf{x}_w$. The well is considered in equation 1 by an internal boundary. The velocity field $\mathbf{v}(\mathbf{x})$ is related to the specific flux by $\mathbf{v}(\mathbf{x}) = \mathbf{q}(\mathbf{x})/n$, where n is the porosity, which is assumed to be constant.

[8] For plane steady state flow conditions, the boundary of a well catchment is identical to the boundary streamline in any realization i. The boundary streamline extends from the stagnation point S_i to the domain boundary or water divide on two branches, provided that a stagnation point exists. By reversing the velocity field to $-\mathbf{v}(\mathbf{x})$ the boundary streamline belongs to the particle trajectory s_i, which starts at the well W (see Figure 1 for homogeneous conditions), passes by the stagnation point S_i, and approaches the upstream boundary or water divide on the two branches $\mathbf{s}_{i,I}$, and $\mathbf{s}_{i,II}$. The uncertainty of the boundary location may be approximately expressed by the transversal second moment of the particle displacements of particles starting at the well W, and passing along the mean trajectories $\mathbf{s}_I(\mathbf{x})$ and $\mathbf{s}_{II}(\mathbf{x})$. This concept was used by *Dagan* [1984] for the expression of preasymptotic macrodispersion effects for uniform mean flow conditions and by *Indelman and Dagan* [1999] for divergent radial flow. However, the mean streamline of a well catchment is much more complex by being curved, and by passing by a stagnation point S. Moreover, the mean velocity along the mean trajectory $\mathbf{s}$ is extremely nonuniform. This effect is amplified by the areal recharge rate N.

[9] We adopt a locally orthogonal coordinate system l, p, with l being the coordinate along the mean streamline $\mathbf{s}(\mathbf{x})$, and p normal to it, starting at the well W (Figure 1) with $l(\mathbf{x}_W) = 0$, $p(\mathbf{x}_W) = 0$. For any realization i the particle location at time t can be expressed by the integral

$$\mathbf{X}(t) = \int_0^t \mathbf{v}(X(t'))dt' \quad (2)$$

where $\mathbf{X}(t)$ is the particle trajectory, $\mathbf{v}(\mathbf{x}(t))$ is the velocity, both at location $\mathbf{x}$ and time t. By adopting the first-order expansion $\mathbf{X}(t) \approx \langle \mathbf{X}(t) \rangle + \mathbf{X}'(t)$, and $\mathbf{v}(\mathbf{X}(t)) \approx \mathbf{U}(\mathbf{X}(t)) + \mathbf{u}(\mathbf{X}(t))$ the particle location and velocity are expressed by their respective mean and deviation. The vector $\mathbf{U}(X(t)) = \langle \mathbf{v}(\mathbf{X}(t)) \rangle$ is the averaged velocity. The symbol $\langle\rangle$ denotes the ensemble mean. Consequently the particle trajectory increment over time is approximated in first order by

$$\frac{d\mathbf{X}'(t)}{dt} \approx \mathbf{u}(\langle \mathbf{X}(t) \rangle) + \frac{\partial \mathbf{U}}{\partial \mathbf{X}'}(\langle \mathbf{X}(t) \rangle)\mathbf{X}'(t) \quad (3)$$

[10] The existence of a stagnation point S on the mean trajectory $\mathbf{s}(\mathbf{x})$ makes it necessary to consider separately the sections from the well to the stagnation point and from the stagnation point to the catchment boundary or water divide (Figure 1). For homogeneous conditions, the streamline arriving at the stagnation point is perpendicular to the two streamlines departing. It is assumed that this concept holds also for heterogeneous conditions in an approximate manner. This orthogonality requires considering on the first section the longitudinal displacement of the particles, whereas for the continuation on the second section the transversal displacement is applicable. Therefore both the longitudinal and the transversal particle trajectories as well as the second moment of the displacements have to be formulated.

2.2. Longitudinal Particle Trajectory and Second Moment in a Curved Locally Orthogonal System

[11] In the curved, locally orthogonal coordinate system l, p, the longitudinal component in equation 3 is locally given in first order approximation by:

$$\frac{dX_l'(t)}{dt} \approx u_l(l) + \frac{\partial U_l}{\partial l}(l)X_l'(l) \quad (4)$$

with $l = l(t)$. Equation 4 holds for symmetric flow conditions around the mean trajectory. It is assumed here that asymmetry effects can be neglected. This assumption will be made in our whole study. Equation 4 can be integrated up to the location $l = L(t)$ adopting the initial condition $X_l(l = 0) = 0$:

$$X_l'(t) \approx U_l(L(t)) \int_0^t \frac{u_l(l(t'))}{U_l(l(t'))}dt = U_l(L(t)) \int_0^{L(t)} \frac{u_l(l)}{U_l^2(l)}dl \quad (5)$$

Based on equation 5 the longitudinal second moment of the particle displacements is approximated by:

$$X_{ll}'(t) \approx U_l^2(L(t)) \int_0^{L(t)} \int_0^{L(t)} \frac{u_{ll}(l', l'')}{U_l^2(l')U_l^2(l'')}dl'dl'' \quad (6)$$

The function $u_{ll}(l',l'')$ is the longitudinal velocity covariance, which is as yet unknown for a nonuniform flow field. For

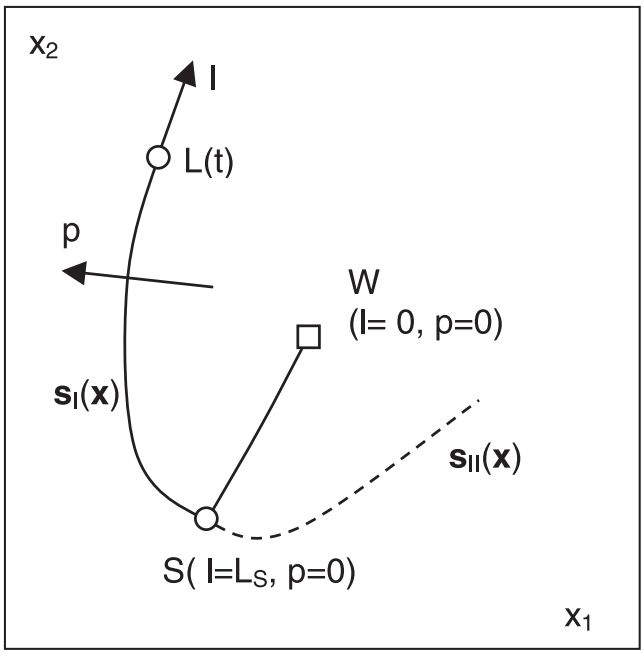

Figure 1. Locally orthogonal coordinate system with longitudinal (l) and perpendicular (p) coordinates of mean particle trajectory for catchment boundary, starting at well W, and passing by the stagnation point S.

uniform mean conditions equation 6 is identical to that obtained by *Indelman and Dagan* [1999] for a Cartesian system (x_1, x_2). Besides the velocity covariance the mean velocity is needed along the mean particle trajectory.

2.3. Transversal Particle Trajectory and Second Moment in a Curved Locally Orthogonal System

[12] The transversal component in equation 3 can be described locally in the curved, locally orthogonal coordinate system l, p by

$$\frac{dX'_p(t)}{dt} \approx u_p(l) + \frac{\partial U_p}{\partial p}(l)X'_l(l) \tag{7}$$

and $l = l(t)$ in a first-order approximation. The partial derivative $\partial U_p/\partial p$ can be expressed using local continuity and assuming constant thickness H by

$$\frac{\partial U_p}{\partial p} = -\frac{\partial U_l}{\partial l} + \frac{N}{Hn} \tag{8}$$

which leads to

$$\frac{dX'_p(t)}{dt} \approx u_p(l) - \left[\frac{\partial U_l}{\partial l}(l) - \frac{N}{Hn}\right]X'_p(l) \tag{9}$$

Equation 9 can be integrated, adopting the initial condition $X_p(l = 0) = 0$:

$$X'_p(t) \approx \frac{1}{U_l(L(t))}\int_0^t u_p(l(t'))\exp\left[\frac{N}{Hn}\cdot(t-t')\right]U_l(l(t'))dt' \tag{10}$$

or:

$$X'_p(t) \approx \frac{1}{U_l(L(t))}\int_0^{L(t)} u_p(l)\exp\left[\frac{N}{Hn}\cdot(t(L)-t'(l))\right]dl \tag{11}$$

Equation 11 is the basis for calculating the transversal second moment of the particle displacements:

$$X'_{pp}(t) \approx \frac{1}{[U_l(L(t))]^2}\int_0^{L(t)}\int_0^{L(t)} u_{pp}(l',l'') \cdot \exp\left[\frac{N}{Hn}\cdot(2t(L)-t(l')-t(l''))\right]dl'dl'' \tag{12}$$

The function $u_{pp}(l', l'')$ is the transversal velocity covariance, also unknown yet for a nonuniform velocity field. Note that equation 12 is valid for constant saturated thickness H. For variable thickness, including unconfined conditions, it can be approximated in the following way:

$$X'_{pp}(t) \approx \frac{1}{[U_l(L(t))]^2}\int_0^{L(t)}\int_0^{L(t)} u_{pp}(l',l'') \cdot \exp\left[\frac{N}{n}\cdot\left(\frac{2t(L)}{H(L)}-\frac{t(l')}{H(l')}-\frac{t(l'')}{H(l'')}\right)\right]dl'dl'' \tag{13}$$

In addition to the velocity covariance and the mean velocity **U**, the recharge rate N, the porosity n, the thickness H, and the average arrival times t(l) of the particles along the mean trajectories are needed. The information required can be obtained by conventional groundwater modeling.

2.4. Velocity Covariance

[13] Expressions for the two-dimensional longitudinal and transversal velocity covariances $u_{ll}(l',l'')$ and $u_{pp}(l',l'')$ are well known for uniform mean velocity fields [*Rubin*, 1990]. Under these conditions they are functions of the variance σ_Y^2, the correlation length I_Y, and the mean velocity U. For general nonuniform flow conditions, however, no general formulation is available. For two-dimensional nonuniform parallel flow conditions with constant recharge rate, *Butera and Tanda* [1999] formulated the velocity covariance based on the head variogram formulation of *Rubin and Dagan* [1987]. Since we aim at an expression of the scaled form $u_{ll}(l',l'')/(U(l')U(l'')\sigma_Y^2)$ and $u_{pp}(l',l'')/(U(l')U(l'')\sigma_Y^2)$ needed in connection with the integration in equations 6 and 13, we reformulate the expression. The result is given in Appendix A. It represents the correction due to the existence of a constant recharge rate. *Butera and Tanda* [1999] found no impact of the recharge on the transversal displacements covariance when comparing solutions with and without considering recharge. It can thus be expected that the use of the transversal velocity covariance for uniform mean flow is precise enough. Therefore the numerical evaluation of the integral in equations 6 and 13 is performed using the scaled velocity covariances $\tilde{u}_{ll}(\mathbf{x},\mathbf{x}')$ and $\tilde{u}_{pp}(\mathbf{x},\mathbf{x}')$ for uniform mean flow. Both covariances are evaluated along the mean trajectory and using the distance $|\mathbf{x} - \mathbf{x}'|$ between the locations $\mathbf{x}$ and $\mathbf{x}'$. Note that in curved

systems this distance is different from the path length. This concept represents a simplification and approximation for generally nonuniform mean flow conditions. In addition to this concept, the velocity covariance correction for nonuniform, parallel mean flow according to the Appendix is incorporated in our analysis as an option.

[14] The above mentioned approximations for the velocity covariances $u_{ll}(l',l'')$ and $u_{pp}(l',l'')$ still require that the location under consideration is far away from the domain boundary. *Rubin and Dagan* [1988, 1989] showed that the presence of boundaries influences the structure of the head variogram along a zone of width up to three correlation lengths I_Y. A similar effect can thus be expected for the velocity covariances. *Osnes* [1998] found these effects for uniform mean flow conditions. The transversal velocity variance evaluated for a rectangular region decreased to zero toward an impermeable or a constant head boundary. Although the flow field near a well is far from being quasi-uniform, we may expect similar effects due to the presence of the domain boundary in a zone along the boundary being up to three correlation lengths I_Y wide.

2.5. Approximation of the Uncertainty Bandwidth for a Well Catchment

[15] The uncertainty of the location of a well catchment boundary is estimated for the boundary streamline starting at the well (Figure 1). For any particle along the catchment boundary the particle trajectory is

$$X'_p(t) \approx U_l(L_S)\int_0^{L_S}\frac{u_l(l)}{U_l^2(l)}dl + \frac{1}{U_l(L(t))}\int_{L_S}^{L(t)} u_p(l)\cdot\exp\left[\frac{N}{Hn}\cdot(t(L)-t(l))\right]dl \qquad (14)$$

[16] The corresponding second moment of the transversal particle trajectory is:

$$X'_{pp}(t) \approx U_l^2(L_S)\int_0^{L_S}\int_0^{L_S}\frac{u_{ll}(l',l'')}{U_l^2(l')U_l^2(l'')}dl'dl'' + \frac{1}{[U_l(L(t))]^2}\cdot\int_{L_S}^{L(t)}\int_{L_S}^{L(t)} u_{pp}(l',l'')\cdot\exp\left[\frac{N}{n}\cdot\left(\frac{2t(L)}{H(L)}-\frac{t(l')}{H(l')}-\frac{t(l'')}{H(l'')}\right)\right]dl'dl'' + 2\frac{U_l(L_S)}{U_l(L(t))}\int_0^{L_S}\int_{L_S}^{L(t)}\frac{u_{lp}(l',l'')}{U_l^2(l')}\cdot\exp\left[\frac{N}{n}\cdot\left(\frac{t(L)}{H(L)}-\frac{t(l'')}{H(l'')}\right)\right]dl'dl'' \qquad (15)$$

The function $u_{lp}(l',l'')$ is the velocity cross-covariance. For the case that the scaled uniform covariance $\tilde{u}_{lp}(l',l'')$ according to *Rubin* [1990] is accepted, it becomes zero along the mean trajectory s(l, p = 0). Therefore the last term in equation 15 vanishes. Consequently the second moment contributions of the two sections can be added up directly.

[17] The evaluation of the first term in equation 15, which represents the longitudinal second moment, yields zero at the stagnation point S. The corresponding transversal second moment would be infinite. Since the stagnation point is a singular point with strongly converging and diverging flow components in its surroundings, it is obviously not possible to evaluate the second moment by equations 6 and 13 for this location. The first-order approximation fails at the stagnation point. As an alternative we use the following (crude) approximation. The contribution of the segment between well and stagnation point is approximated empirically. It is based on the longitudinal second moment for radial mean flow conditions [after *Indelman and Dagan*, 1999], for which we can use their analytical approximation:

$$X'_{rr}(t) \approx \sigma_Y^2 I_Y\cdot\left\{\frac{2\tilde{r}}{3}-1-\frac{2}{\tilde{r}^2}\cdot[(1+\tilde{r})\exp(-\tilde{r})-1]\right\} \qquad (16)$$

with $\tilde{r} = L(t)/I_Y$. Based on this equation, the lateral second moment at the stagnation point L_s is approximated empirically by:

$$X'_{ll}(t(L_S)) \approx X'_{rr}(t(L_S))\cdot\left(1-\frac{1}{2}\frac{Q_w}{Nw^2}\right) \qquad (17)$$

[18] The parameter w is the distance from the well to the upstream boundary or water divide. The empirical correction in equation 17 accounts for the effect of the extremely diverging flow field near the stagnation point. The dimensionless term $Q' = Q_w/(N\,w^2)$ [*Kinzelbach et al.*, 1992] is a measure of the relative well discharge rate, or for the relative catchment area, and therefore also for the relative catchment width. For high pumping rates this width is large, and therefore the impact of the extremely diverging flow field is large, compared to low pumping rates. The applicability of this procedure is restricted to values of $Q'<2$. Note that equation 17 only estimates the initial lateral second moment of the particle displacement at the stagnation point.

[19] The numerical evaluation of equation 13 is straightforward. The integral is approximated by the double sum over finite segments Δl, which are nothing else than the particle tracking steps for mean flow conditions. The variables U(l) and H(l) are taken at the location l(t) along the catchment boundary **s** of the mean flow model, which is solved either analytically if possible, or numerically.

[20] By assuming a Gaussian distribution of the transversal particle displacement variance X'_{pp} the probability density of the location of the catchment boundary is given. By taking an uncertainty bandwidth corresponding to twice the standard deviation $\sqrt{X_{pp}}$ on both sides of the mean trajectory **s(x)**, a 95% confidence interval for the location of the catchment boundary is estimated.

[21] The presence of boundaries of any type will undoubtedly affect the uncertainty bandwidth. This concerns not only the lateral boundaries but also the upstream boundary or water divide. Besides the boundary effect of the velocity covariance the existence of a boundary affects the probability density of the catchment boundary, which can no longer be approximated by a Gaussian distribution. Impermeable boundaries and water divides are streamlines. The catchment boundary approaches this streamline asymptotically. Therefore the validity of the present analysis is limited to the region, which is sufficiently far away from the boundary or water divide.

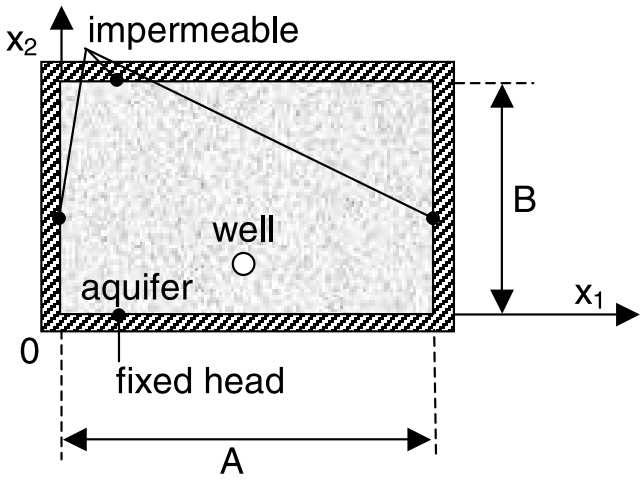

Figure 2. Aquifer domain of rectangular test cases with uniform recharge rate and constant pumping rate.

[22] For comparison, the stochastic Lagrangian approximation method is applied to a set of examples defined in 4.1 and compared with the results of Monte Carlo simulations.

3. Numerical Simulation of the Well Catchment Boundary Distribution

[23] The procedure for the stochastic numerical evaluation of the uncertainty of the well catchment boundary according to a Monte Carlo technique is as follows.

1. Generation of a set of m realizations of Y = ln(K) fields for a rectangular grid given the variance and correlation length of Y using the code FGEN96 version 9.21 [*Robin et al.*, 1993; *Robin and Schmidt*, 1996].

2. Calculation of the steady state velocity field $\mathbf{v}_i(\mathbf{x})$ for each realization using MODFLOW [*U.S. Geological Survey*, 1996] for a rectangular grid. The calculation leads to the fluxes through the cell faces.

3. Searching for the stagnation point S_i in the vicinity of the well by checking the cell velocity and starting the particle tracking from the two locations in the neighborhood of S_i, for every realization, given a time step increment. The particle tracking uses the velocity interpolation after Pollock and the time integration according to the second-order Runge-Kutta method [*Kinzelbach et al.*, 1992]. It is based on the cell fluxes. A check is made whether the starting positions lead to tracks, which cover both branches of the catchment.

4. Analysis of the particle tracks of all realizations in a predefined grid by testing whether a considered cell belongs to the catchment. This yields a probability map showing the probability of a particular point being inside the catchment.

4. Application and Comparison of Results

4.1. Test Cases

[24] The semianalytical and numerical procedures described above are applied to a set of synthetic test cases, which do not depend on local data. The cases comprise a single well with areal recharge (Figure 2). The domain is a rectangular, two-dimensional unconfined heterogeneous aquifer with horizontal impermeable base. The spatial variability of the aquifer's hydraulic conductivity $K(\mathbf{x})$ is given by the variance and the correlation length of Y = ln(K). The three boundaries ($x_1 = 0$, x_2, western boundary), ($x_1 = A$, x_2, eastern boundary), and (x_1, $x_2 = B$, northern boundary) are impermeable. The boundary (x_1, $x_2 = 0$, southern boundary) is a boundary with fixed head at a level $h(x_1, x_2 = 0) = h_0$. Without well a nonuniform flow is in north-south direction toward the fixed-head boundary. The input parameters of the examples are presented in Table 1. The examples allow a demonstration of the impact of lateral boundaries, of increased variance of Y, and of reduced well discharge rate. They comprise simplified, but nevertheless typical conditions for relatively small and highly conductive unconfined aquifers. Such conditions with a quasi-steady state flow field are often found in Central Europe. A variance σ_Y^2 between 0.1 and 1 is typical for vertically averaged plane aquifers. A correlation length of 100m corresponds to a fraction of 1/10 of the distance between the well and the upstream boundary.

[25] For the semianalytical approach according to section 2, the flow field is calculated analytically. For the particle tracking, a backward Runge-Kutta scheme is used with a spatial increment of $\Delta s = 10$ m. For the numerical modeling according to section 3, a discretization with a mesh size of 10 m and a time step of 30d is used.

4.2. Comparison of Results

[26] The Monte Carlo type simulation results are presented as a map of the probability of a given point $\mathbf{x}$ belonging to the well catchment (Figures 3a–6a). The lines

Table 1. Input Parameters for Test Cases

	Experiment 1	Experiment 2	Experiment 3	Experiment 4
Well discharge rate Q_W [m^3/d]	432	432	432	216
Recharge rate N [mm/d]	1	1	1	1
Geom. mean Hydraulic conductivity K [m/d]	432	432	432	432
Variance of Y = ln(K) [-]	0.1	0.1	1	0.1
Correlation length of Y (integral scale) [m]	100	100	100	100
Porosity n [-]	0.1	0.1	0.1	0.1
Length A of domain in x_1 direction [m]	2000	1000	2000	2000
Width B of domain in x_2 direction [m]	1200	1000	1200	1200
Coordinate x_1 of well [m]	995	495	995	995
Coordinate x_2 of well [m]	505	305	505	505
Constant head h_0 [m]	10	10	10	10

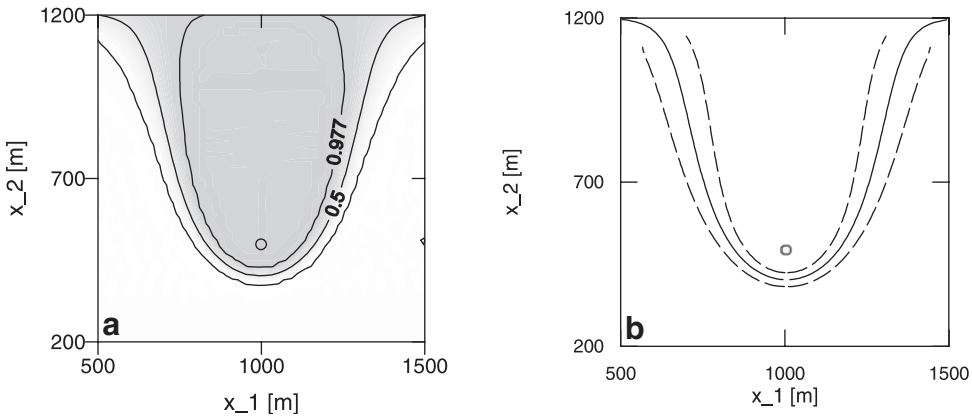

Figure 3. Uncertainty bandwidth (95%) of well catchment boundary, example 1; cut from flow domain 2000 m × 1200 m; well at x_1 = 995 m, x_2 = 505 m; well discharge rate Q_W = 432 m^3/d; recharge rate N = 1 mm/d; variance σ_Y^2 = 0.1, correlation length I_Y = 100 m. (a) Monte Carlo simulation with 1000 realizations; dark shading, probability 1; no shading, probability 0 to belong to well catchment. (b) Semianalytical approach.

of equal probability 0.977, 0.5 and 0.023 correspond to the uncertainty bandwidth of the semianalytical approach (Figures 3b–6b). Figure 3a represents the standard case. The impact of relatively close lateral boundaries is demonstrated in Figure 4a. It mainly affects the shape of the mean catchment boundary together with the uncertainty bandwidth near the upstream boundary. The influence of an increase in the variance of Y by a factor of 10 is shown in Figure 5a. A reduction of the well discharge rate to 50% leads to the probability map presented in Figure 6a. An analysis of the realizations shows that 1000 Monte Carlo runs are sufficient to present stable ensemble statistics.

[27] The results of the semianalytical approach (Figures 3b–6b) are quite similar to the Monte Carlo type results except for the uncertainty bandwidth near the upstream boundary. The catchment boundary for homogeneous conditions is practically identical to the 50% boundary over all realizations. The uncertainty bandwidth clearly deviates from the numerical results within a zone of about two correlation lengths from the upstream boundary. The initial uncertainty bandwidth near the stagnation point is represented relatively well in most cases. The impact of lateral boundaries, as shown in Figure 4, is visible in an overestimation of the bandwidth compared to the numerical results.

5. Discussion and Conclusions

[28] In this paper we present a first-order analytical approximation for expressing the covariance of the particle displacements in a spatially variable, steady state, nonuniform mean flow field. Based on a semianalytical evaluation of this covariance, the uncertainty of the location of the catchment boundary for pumping wells is estimated. The evaluation of the uncertainty bandwidth is of practical use, since only few observations are usually available. The presence of heterogeneities in the hydraulic conductivity field may strongly affect the uncertainty bandwidth. The semianalytical results are obtained with a computational

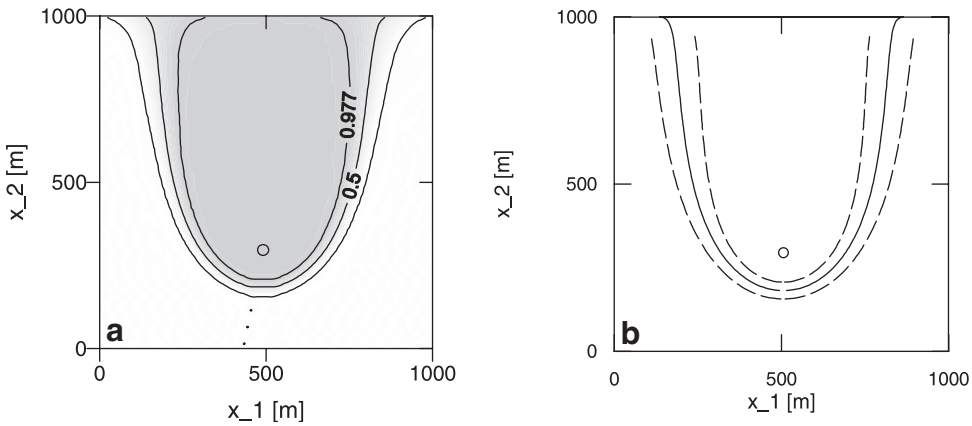

Figure 4. Uncertainty bandwidth (95%) of well catchment boundary, example 2; flow domain 1000 m × 1000 m; well at x_1 = 495 m, x_2 = 305 m; well discharge rate Q_W = 432 m^3/d; recharge rate N = 1 mm/d; variance σ_Y^2 = 0.1, correlation length I_Y = 100 m. (a) Monte Carlo simulation with 1000 realizations; dark shading, probability 1; no shading, probability 0 to belong to well catchment. (b) Semianalytical approach.

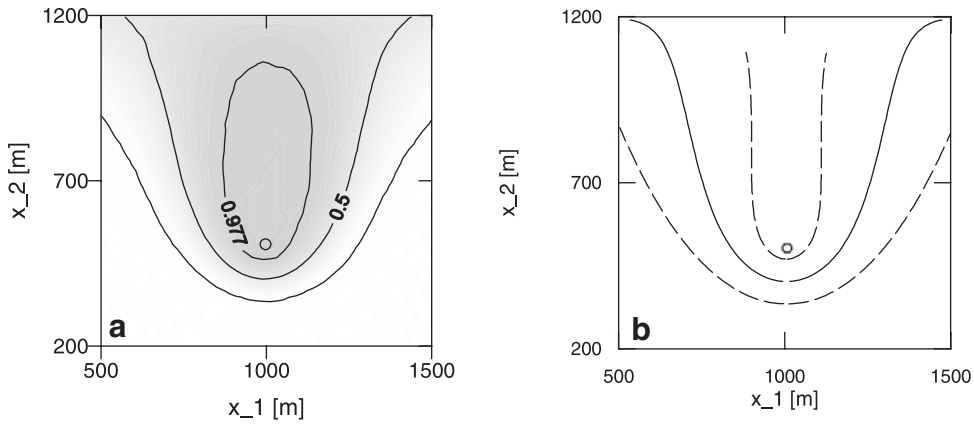

Figure 5. Uncertainty bandwidth (95%) of well catchment boundary, example 3, cut from flow domain 2000 m × 1200 m; well at x_1 = 995 m, x_2 = 505 m; well discharge rate Q_W = 432 m^3/d; recharge rate N = 1 mm/d; variance σ_Y^2 = 1, correlation length I_Y = 100 m. (a) Monte Carlo simulation with 924 realizations; dark shading, probability 1; no shading, probability 0 to belong to well catchment. (b) Semianalytical approach.

time several orders of magnitude smaller than that of the numerical Monte Carlo method. The method is therefore highly attractive for practical applications.

[29] The comparison of the semianalytical results with the Monte Carlo type simulations shows that the method yields reasonable estimates of the uncertainty bandwidth. Maximum deviations in the bandwidth from the numerical results are in the order of 5 to 50%. The largest deviations in the uncertainty bandwidth are obtained for upstream and lateral boundaries less than about two correlation lengths away from the mean catchment boundary location. The reason for the latter is mainly due to an alteration of the velocity covariance near boundaries. However, no reasonable estimates for velocity covariance in nonuniform flow fields near a domain boundary are available. Therefore in the vicinity of boundaries the application of the semianalytical results is limited to a minimum distance of about two correlation lengths from the domain boundary.

[30] A weak point in the present semianalytical approach is the empirical estimation of the initial second lateral moment near the stagnation point by using equation 17. Up to now, no reasonable alternative was found to circumvent the difficulties using equations 6 and 13 near the stagnation point, which is believed to be caused by the extremely diverging velocity field. A possible explanation of the difficulties could be a limitation due to the first-order perturbation used in the development of the method. A further limitation originates from the evaluation of the velocity covariance in nonuniform flow fields. The impact of the curved mean particle trajectory on the estimate of the lateral second moment is an additional source of error. However, compared with the two problems described above, it is believed to be of second-order significance. Overall, the semianalytical Lagrangian approach yields reasonable estimates of the uncertainty bandwidth of the location of the catchment boundary of pumping wells.

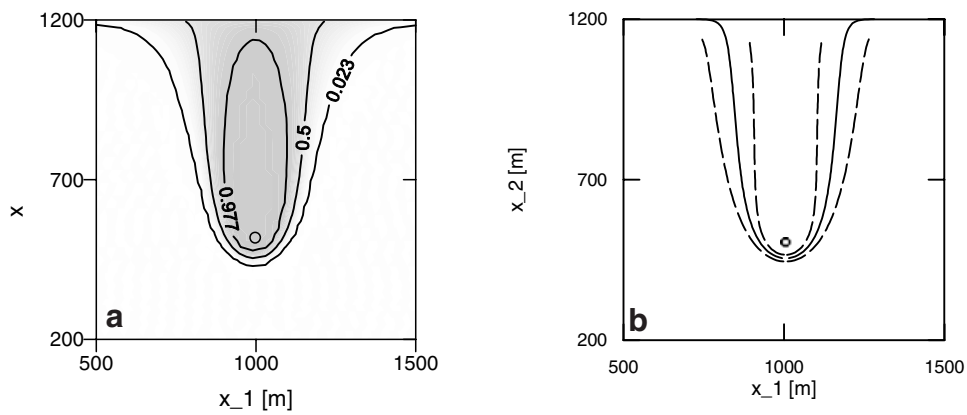

Figure 6. Uncertainty bandwidth (95%) of well catchment boundary, example 4, cut from flow domain 2000 m × 1200 m; well at x_1 = 995 m, x_2 = 505 m; well discharge rate Q_W = 216 m^3/d; recharge rate N = 1 mm/d; variance σ_Y^2 = 0.1, correlation length I_Y = 100 m. (a) Monte Carlo simulation with 1000 realizations; dark shading, probability 1; no shading, probability 0 to belong to well catchment. (b) Semianalytical approach.

Appendix A

A1. Longitudinal Velocity Covariance With Recharge in Two-Dimensional Parallel Flow

$$\frac{u_{11}(\mathbf{x},\mathbf{x}')}{U(\mathbf{x})U(\mathbf{x}')\sigma_Y^2} = \tilde{u}_{11}(\mathbf{x},\mathbf{x}') + \frac{I_Y^2 N^2}{U(\mathbf{x})U(\mathbf{x}')H^2} \cdot \left\{ e^{-r} \cdot \left[-\alpha_1' r^2 + (2\alpha_1' - \alpha_3') + (2\alpha_1' - \alpha_2')r + \frac{(2\alpha_2' - 2\alpha_3' - \alpha_5')}{r} - \frac{3\alpha_5'}{r^2} \right] + 2\alpha_4' + \frac{3\alpha_5'}{r^2} \right\}$$

with $\mathbf{x}$, $\mathbf{x}'$ and $r = |\mathbf{x} - \mathbf{x}'|$, along the mean trajectory, and the constants:

$$\alpha_1' = \frac{3}{32}; \quad \alpha_2' = \frac{13}{32}; \quad \alpha_3' = \frac{25}{32}; \quad \alpha_4' = -\frac{7}{64}; \quad \alpha_1' = 38$$

The function $\tilde{u}_{11}(\mathbf{x}, \mathbf{x}')$ is the scaled longitudinal velocity covariance for uniform mean flow conditions [*Rubin*, 1990].

A2. Transversal Velocity Covariance With Recharge in Two-Dimensional Parallel Flow

$$\frac{u_{22}(\mathbf{x},\mathbf{x}')}{U(\mathbf{x})U(\mathbf{x}')\sigma_Y^2} = \tilde{u}_{22}(\mathbf{x},\mathbf{x}') + \frac{I_Y^2 N^2}{U(\mathbf{x})U(\mathbf{x}')H^2} \cdot \left\{ e^{-r} \cdot \left[-2\alpha_1' + \alpha_2 - \alpha_1' r - \frac{\alpha_2' + \alpha_3'}{r} + \frac{\alpha_5'}{r^2} \right] - 2\alpha_4' - \frac{\alpha_5'}{r^2} \right\}$$

with $\mathbf{x}$, $\mathbf{x}'$ and r again along the mean trajectory, and $\tilde{u}_{22}(\mathbf{x}, \mathbf{x}')$ being the scaled transversal velocity covariance for uniform mean flow conditions [*Rubin*, 1990].

[31] **Acknowledgments.** The study was performed within the European Research Project "Stochastic Analysis of Wellhead Protection and Risk Assessment" W-SAHaRA. This project has been supported by the Swiss Federal Office for Education and Science (BBT), project BBW 99.0543.

References

Butera, I., and M. G. Tanda, Solute transport analysis through heterogeneous media in nonuniform in the average flow by a stochastic approach, *Transp. Porous Media*, *36*(3), 255–291, 1999.

Dagan, G., Solute transport in heterogeneous porous formations, *J. Fluid Mech.*, *145*, 151–177, 1984.

Feyen, L., K. J. Beven, F. De Smedt, and J. Freer, Stochastic capture zone delineation within the generalized likelihood uncertainty estimation methodology: Conditioning on head observations, *Water Resour. Res.*, *37*(3), 625–638, 2001.

Franzetti, S., and A. Guadagnini, Probabilistic estimation of well catchments in heterogeneous aquifers, *J. Hydrol.*, *174*(1–2), 149–171, 1996.

Guadagnini, A., and S. Franzetti, Time-related capture zones for contaminants in randomly heterogeneous formations, *Ground Water*, *37*(2), 253–260, 1999.

Indelman, P., and G. Dagan, Solute transport in divergent radial flow through heterogeneous porous media, *J. Fluid Mech.*, *384*, 159–182, 1999.

Kinzelbach, W., M. Marburger, and M. Chiang, Determination of groundwater catchment areas in two and three spatial dimensions, *J. Hydrol.*, *134*, 221–246, 1992.

Osnes, H., Stochastic analysis of velocity spatial variability in bounded rectangular heterogeneous aquifers, *Adv. Water Resour.*, *21*(1), 203–215, 1998.

Riva, M., A. Guadagnini, and F. Ballio, Time-related capture zones for radial flow in two dimensional randomly heterogeneous media, *Stochastic Environ. Res. Risk Assess.*, *13*(3), 217–230, 1999.

Robin, M. J. L., and R. T. Schmidt, FGEN96 version 9.21, Waterloo Cent. for Groundwater Res., Univ. of Waterloo, Waterloo, Ontario, Canada, 1996.

Robin, M. J. L., A. L. Gutjahr, E. A. Sudicky, and J. L. Wilson, Cross-correlated random field generation with the direct Fourier transform method, *Water Resour. Res.*, *29*(7), 2385–2397, 1993.

Rubin, Y., Stochastic modeling of macrodispersion in heterogeneous porous media, *Water Resour. Res.*, *26*(1), 133–141, 1990, (Correction, *Water Resour. Res.*, *26*(10), 2631, 1990.)

Rubin, Y., and G. Dagan, Stochastic identification of transmissivity and effective recharge in steady state groundwater flow, 1, Theory, *Water Resour. Res.*, *23*(7), 1185–1192, 1987.

Rubin, Y., and G. Dagan, Stochastic analysis of boundaries effects on head spatial variability in heterogeneous aquifers, 1, Constant head boundary, *Water Resour. Res.*, *24*(10), 1689–1697, 1988.

Rubin, Y., and G. Dagan, Stochastic analysis of boundaries effects on head spatial variability in heterogeneous aquifers, 2, Impervious boundary, *Water Resour. Res.*, *25*(4), 707–712, 1989.

U.S. Geological Survey, User's documentation for MODFLOW-96, an update to the U.S. Geological Survey Modular Finite-Difference Ground-Water Flow Model, *U.S. Geol. Surv. Open File Rep., 96-485*, 1996.

van Leeuwen, M., A. P. Butler, C. B. M. te Stroet, and J. A. Tompkins, Stochastic determination of well capture zones, *Water Resour. Res.*, *34*(9), 2215–2223, 1998.

van Leeuwen, M., A. P. Butler, C. B. M. te Stroet, and J. A. Tompkins, Stochastic determination of well capture zones conditioned on regular grids of transmissivity measurements, *Water Resour. Res.*, *36*(4), 949–957, 2000.

Varljen, M. D., and J. M. Schafer, Assessment of uncertainty in time related capture zones using conditional simulation of hydraulic conductivity, *Ground Water*, *29*(5), 737–748, 1991.

Vassolo, S., W. Kinzelbach, and W. Schäfer, Determination of a well head protection zone by stochastic inverse modelling, *J. Hydrol.*, *206*(3/4), 268–280, 1998.

S. Attinger, W. Kinzelbach, F. Stauffer, and S. Zimmermann, Institute of Hydromechanics and Water Resources Management, ETH Zurich, 8093 Zurich, Switzerland. (stauffer@ihw.baug.ethz.ch)